Supplementary Information

Ternary Phosphine Oxide Host Featuring Thermally Activated Delayed Fluorescence for Blue PHOLEDs with > 20% EQE and Extremely Low Roll-offs

*Chenyu Li, Xuefeng Fan, Chunmiao Han and Hui Xu**

Key Laboratory of Functional Inorganic Material Chemistry, Ministry of Education & School of Chemistry and Material Science, Heilongjiang University, 74 Xuefu Road, Harbin 150080, P. R. China

Content

Experimental section

Measurements and Instruments

^{1}H NMR spectra were recorded using a Varian Mercury plus 400NB spectrometer relative to tetramethylsilane (TMS) as internal standard. Molecular masses were determined by a MALDI-TOF-MS. Elemental analyses were performed on a Vario EL III elemental analyzer. The crystal suitable for single-crystal XRD analysis was obtained through slowly diffusing hexane into dichloromethane solution of **DPDPOTZ** and **DCDPOTZ** at room temperature. All diffraction data were collected at 295 K on a Rigaku Xcalibur E diffractometer with graphite monochromatized Mo Kα (λ = 0.71073 Å) radiation in ω scan mode. All structures were solved by direct method and difference Fourier syntheses. Non-hydrogen atoms were refined by full-matrix least-squares techniques on F2 with anisotropic thermal parameters. The hydrogen atoms attached to carbons were placed in calculated positions with C−H = 0.93 Å and U(H) = 1.2Ueq(C) in the riding model approximation. All calculations were carried out with the SHELXL97 program. Absorption and photoluminescence (PL) emission spectra of the target compound were measured using a SHIMADZU UV-3150 spectrophotometer and a SHIMADZU RF-5301PC spectrophotometer, respectively. Raman spectroscopy measurements were carried out on confocal microprobe Raman spectrometer (LabRAM HR800, Horiba Jobin Yvon) with the excitation wavelength of 458 nm laser line at room temperature. Thermogravimetric analysis (TGA) and differential scanning calorimetry (DSC) were performed on Shimadzu DSC-60A and DTG-60A thermal analyzers under nitrogen atmosphere at a heating rate of 10 °C min^{-1}. The morphological characteristics of the *vacuum*-evaporated films were measured with an atom force microscope (AFM) Agilent 5100 under the tapping mode. Cyclic voltammetric (CV) studies were conducted using an Eco Chemie B. V. AUTOLAB potentiostat in a typical three-electrode cell with a glassy carbon working electrode, a platinum wire counter electrode, and a silver/silver chloride (Ag/AgCl) reference electrode. All electrochemical experiments were carried

out under a nitrogen atmosphere at room temperature in dichloromethane. Phosphorescence spectra were measured in dichloromethane using an Edinburgh FPLS 920 fluorescence spectrophotometer at 77 K cooling by liquid nitrogen with a delay of 300 μs using Time-Correlated Single Photon Counting (TCSPC) method with a microsecond pulsed Xenon light source for 10 μs-10 s lifetime measurement, the synchronization photomultiplier for signal collection and the Multi-Channel Scaling Mode of the PCS900 fast counter PC plug-in card for data processing. The TADF dye doped films (100 nm) were prepared through vacuum evaporation for optical analysis and AFM measurement. Photoluminescence quantum yields (PLQY) of these films were measured through a labsphere 1-M-2 (ϕ = 6") integrating sphere coated by Benflect with efficient light reflection in a wide range of 200-1600 nm, which was integrated with FPLS 920. The absolute η_{PL} determination of the sample was performed by two spectral (emission) scans, with the emission monochromator scanning over the Rayleigh scattered light from the sample and from a blank substrate. The first spectrum recorded the scattered light and the emission of the sample, and the second spectrum contained the scattered light of Benflect coating. The integration and subtraction of the scattered light parts in these two spectra arrived at the photon number absorbed by the samples (N_a); while, integration of the emission of the samples to calculate the emissive photon number (N_e). Then, the absolute η_{PL} can be estimated according to the equation of PLQY = N_e/N_a. Spectral correction (emission arm) was applied to the raw data after background subtraction, and from these spectrally corrected curves the quantum yield was calculated using aF900 software wizard.

DFT Calculations

DFT computations were carried out with different parameters for structure optimizations and vibration analyses. The ground (S_0) and the T_1 states of ***m*CP**, **DPDPOTZ** and **DCDPOTZ** in vacuum were optimized by the restricted and unrestricted formalism of Beck's three-parameter hybrid exchange functional[1] and Lee, and Yang and Parr correlation functional[2] B3LYP/6-31G(d,p), respectively. The fully

optimized stationary points were further characterized by harmonic vibrational frequency analysis to ensure that real local minima had been found without imaginary vibrational frequency. The total energies were also corrected by zero-point energy both for the ground state and triplet state. Natural transition orbital (NTO) analysis was performed on the basis of optimized ground-state geometries at the level of B3LYP/6-31G(d,p). [3] The contours were visualized with Gaussview 5.0. All computations were performed using the Gaussian 09 package. [4]

Device Fabrication and Testing

Before loading into a deposition chamber, the ITO substrate was cleaned with detergents and deionized water, dried in an oven at 120 °C for 4 h, and treated with oxygen plasma for 3 min. Devices were fabricated by evaporating organic layers at a rate of 0.1-0.2 nm s^{-1} onto the ITO substrate sequentially at a pressure below 4×10^{-4} Pa. Onto the electron-transporting layer, a layer of LiF with 1 nm thickness was deposited at a rate of 0.1 nm s^{-1} to improve electron injection. Finally, a 100-nm-thick layer of Al was deposited at a rate of 0.6 nm s^{-1} as the cathode. The emission area of the devices was 0.09 cm^2 as determined by the overlap area of the anode and the cathode. After fabrication, the devices were immediately transferred to a glove box for encapsulation with glass cover slips using epoxy glue. The EL spectra and CIE coordinates were measured using a PR655 spectra colorimeter. The current density-voltage and brightness–voltage curves of the devices were measured using a Keithley 4200 source meter and a calibrated silicon photodiode. All the measurements were carried out at room temperature under ambient conditions. For each structure, four devices were fabricated in parallel to confirm the performance repeatability. To make conclusions reliable, the data reported herein were most close to the average results.

Single Crystal Structure of DPDPOTZ and DCDPOTZ

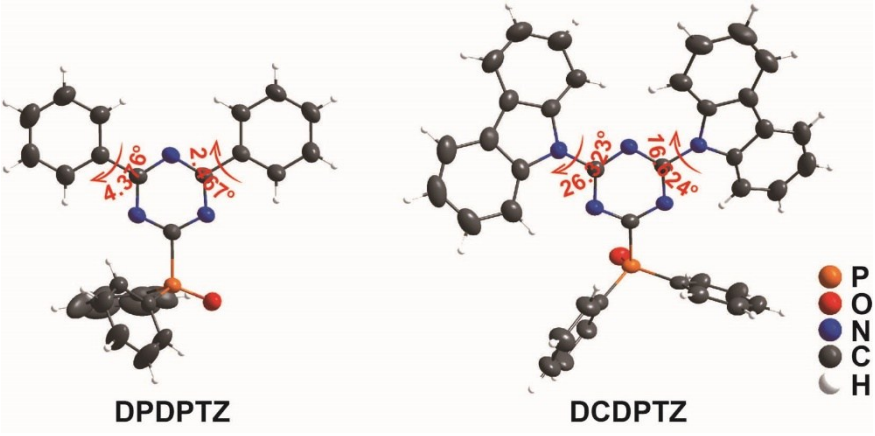

Figure S1. Molecular configuration of **DPDPOTZ** and **DCDPOTZ** obtained by single-crystal X-ray diffraction results.

Thermal Properties of DPDPOTZ and DCDPOTZ

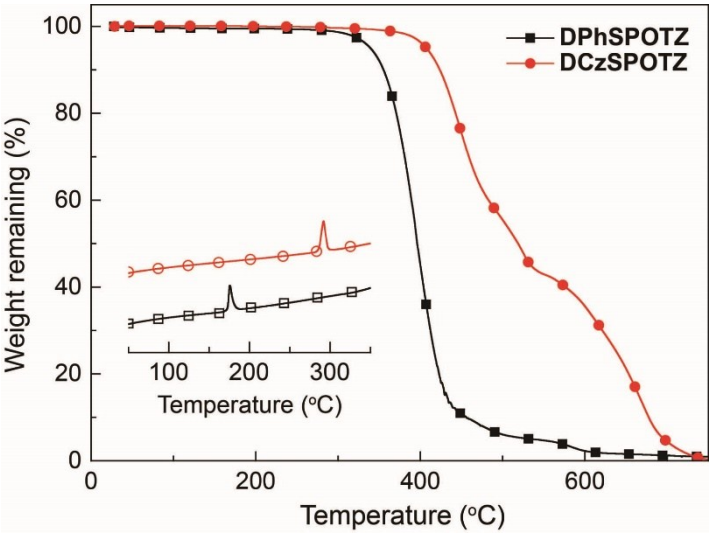

Figure S2. Difference scanning calorimetry (DSC, inset) and thermal gravity analysis (TGA) curves of **DPDPOTZ** and **DCDPOTZ**.

DFT Results of DPDPOTZ and DCDPOTZ

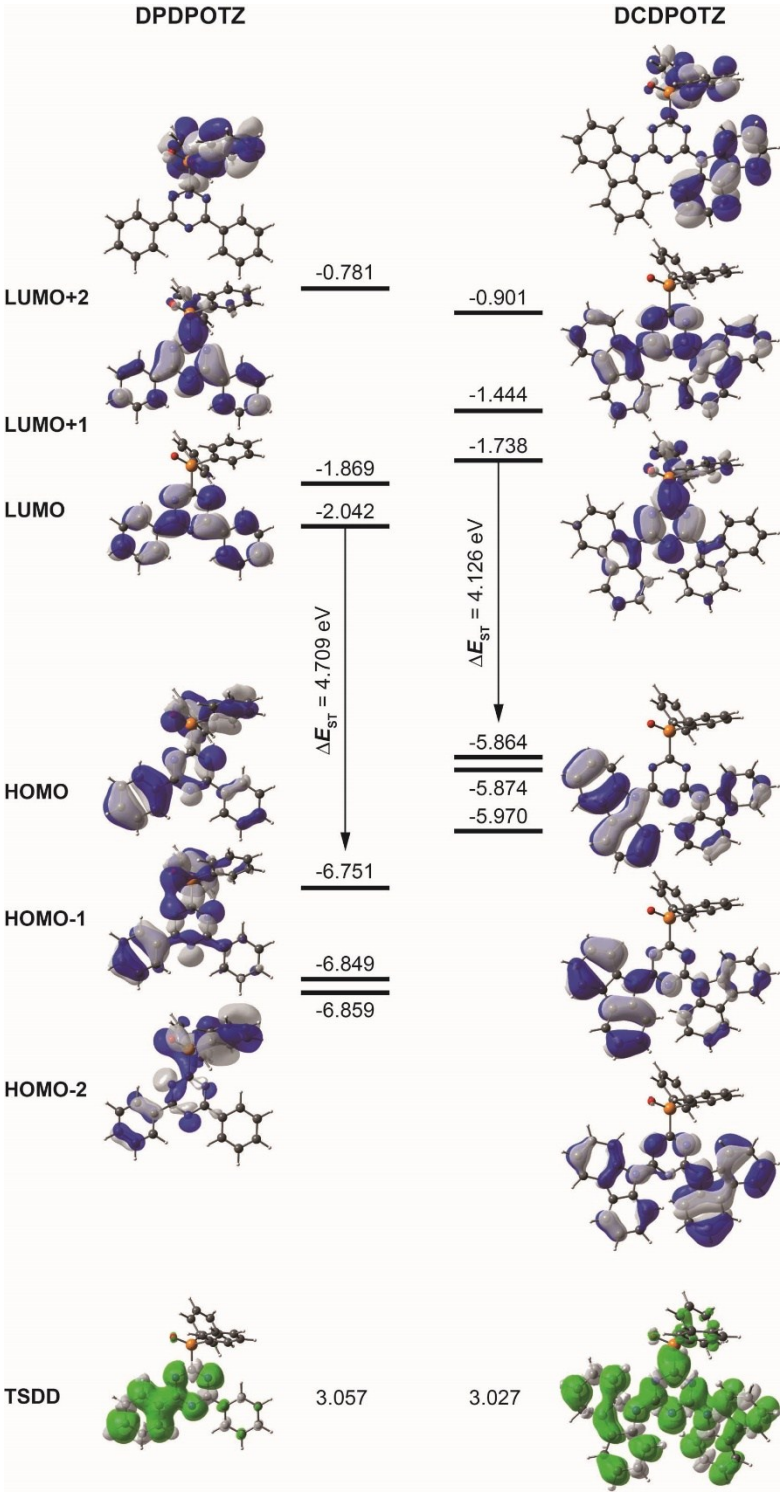

Figure S3. Energy levels and contours of the frontier molecular orbitals and the T_1 states for **DPDPOTZ** and **DCDPOTZ** simulated with DFT calculation. The T_1 locations were indicated with spin density distributions.

PL spectrum of FIr6-doped DPDPOTZ and DCDPOTZ Films

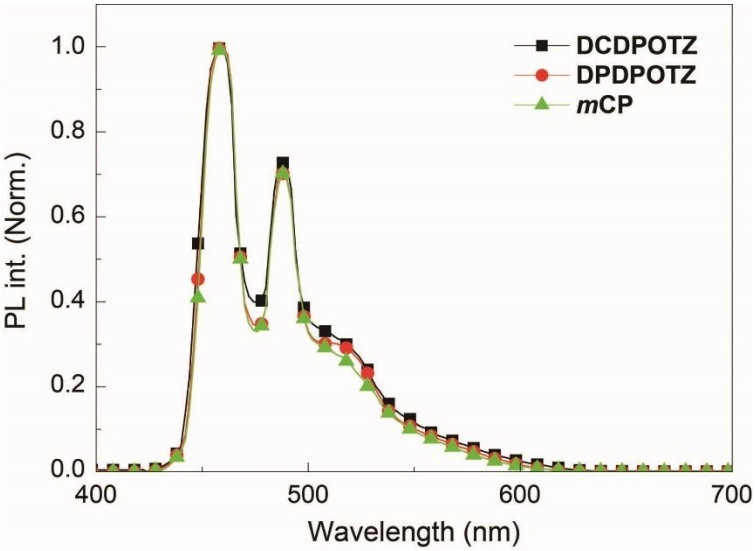

Figure S4. PL spectrum of vacuum-evaporated FIr6-doped **DPDPOTZ**, **DCDPOTZ** and *m*CP films (10 wt%, 100 nm).

Table S1. Photophysical properties of DPDPOTZ and DCDPOTZ.

Compound	λ_{abs} (nm)	λ_{em} (nm)	S_1/T_1 (eV)	ΔE_{ST} (eV)	η_{PL}[g] (%)	HOMO (eV)	LUMO (eV)	T_m/T_d (°C)	μ_e/μ_h[i] (10^{-5} cm^2 V^{-1} s^{-1})
DPDPOTZ	228,276[a]	348, 365, 380[a]	3.88[d]/2.95[e]	0.93[a]	75[b]	-6.74[h]	-3.41[h]	176/342	3.8/0.05
	232, 285[b]	/400[b]	4.17[f]/3.07[f]	1.10[f]	53[c]	-6.75[f]	-2.04[f]		
DCDPOTZ	228, 282, 332[a]	420[a]/433[b]	3.20[d]/2.93[e]	0.27[a]	92[b]	-6.29[h]	-3.41[h]	292/412	2.6/1.8
	232, 286, 338[b]	/460, 488[c]	3.56[f]/3.05[f]	0.51[f]	91[c]	-5.86[f]	-1.74[f]		

[a] In CH_2Cl_2 (10^{-6} mol L^{-1}); [b] doped in DPEPO films (10%wt.); [c] doped with FIr6 (10%wt.); [d] estimated according to the fluorescence spectra; [e] calculated according to PH emissions; [f] Gaussian simulation results; [g] photoluminescence quantum yield (PLQY) measured with integrated sphere; [h] estimated according to the equation HOMO/LUMO = 4.78 + onset voltage; [i] electron and hole mobility estimated according to field-dependent space charge limited current (SCLC) mode.

EQE vs. Luminance Curves

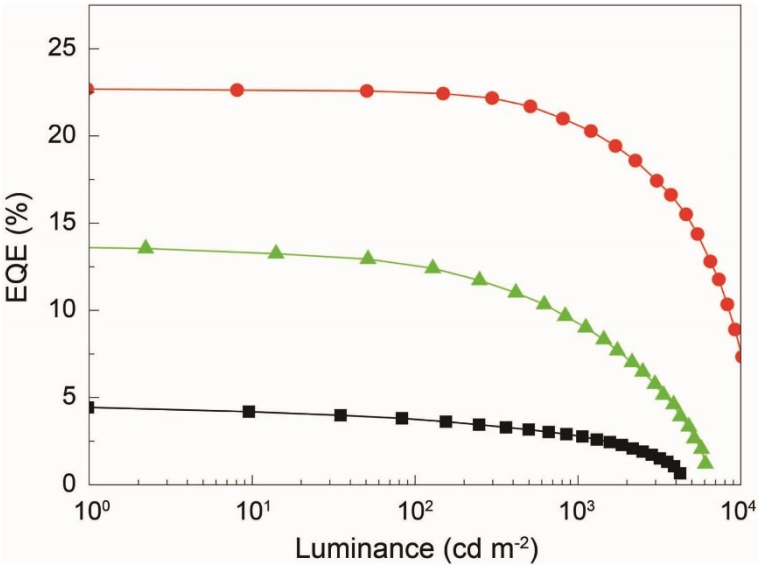

Figure S5. EQE-Luminance curves of **DPDPOTZ** (black), **DCDPOTZ** (red) and *m*CP (green) based devices.

Table S2. EL performance of FIr6-based OLEDs.

Host	Voltage[a] (V)	L_{max} (cd m^{-2})	Max. Efficiencies[b]	Efficiency roll-offs[c] (%)			CIE (x, y)
				CE	PE	EQE	
DPDPOTZ	3.0, 5.0, 8.0	4239	7.2, .7.5, 4.4	18, 38	51, 77	18, 38	(0.15, 0.25)
DCDPOTZ	2.8, 4.3, 6.3	12133	36.6, 41.8, 22.9	1, 11	36, 61	1, 11	(0.15, 0.25)
***m*CP**	3.8, 5.3, 7.8	6064	22.0, 21.3, 13.7	9, 34	44, 72	9, 34	(0.15, 0.26)

[a] In the order of onset, 100 and 1000 cd m^{-2}; [b] in the order of CE (cd A^{-1}), PE (lm W^{-1}) and EQE (%); [c] in the order of 100 and 1000 cd m^{-2}.

References

1. A. D. Becke, *J. Chem. Phys.*, 1993, **98**, 5648-5652.
2. C. Lee, W. Yang and R. G. Parr, *Phys. Rev. B*, 1988, **37**, 785-789.
3. R. L. Martin, *J. Chem. Phys.*, 2003, **118**, 4775-4777.
4. M. J. Frisch, G. W. Trucks, H. B. Schlegel, G. E. Scuseria, M. A. Robb, J. R. Cheeseman, G. Scalmani, V. Barone, B. Mennucci, G. A. Petersson, H. Nakatsuji, M. Caricato, X. Li, H. P. Hratchian, A. F. Izmaylov, J. Bloino, G. Zheng, J. L. Sonnenberg, M. Hada, M. Ehara, K. Toyota, R. Fukuda, J. Hasegawa, M. Ishida, T. Nakajima, Y. Honda, O. Kitao, H. Nakai, T. Vreven, J. A. Montgomery, J. E. Peralta, F. Ogliaro, M. Bearpark, J. J. Heyd, E. Brothers, K. N. Kudin, V. N. Staroverov, R. Kobayashi, J. Normand, K. Raghavachari, A. Rendell, J. C. Burant, S. S. Iyengar, J. Tomasi, M. Cossi, N. Rega, J. M. Millam, M. Klene, J. E. Knox, J. B. Cross, V. Bakken, C. Adamo, J. Jaramillo, R. Gomperts, R. E. Stratmann, O. Yazyev, A. J. Austin, R. Cammi, C. Pomelli, J. W. Ochterski, R. L. Martin, K. Morokuma, V. G. Zakrzewski, G. A. Voth, P. Salvador, J. J. Dannenberg, S. Dapprich, A. D. Daniels, Ö. Farkas, J. B. Foresman, J. V. Ortiz, J. Cioslowski and D. J. Fox, *Gassian Co.*, 2009.